TRI–PP–99–28
Sept 1999

NUCLEON-NUCLEON PARITY VIOLATION EXPERIMENTS*

WILLEM T.H. VAN OERS†
Institut für Kernphysik, Forschungszentrum Jülich,
D-52425 Jülich, Germany
and
Department of Physics, University of Manitoba,
Winnipeg, MB, Canada R3T 2N2
and
TRIUMF, 4004 Wesbrook Mall, Vancouver, B.C.,
Canada V6T 2A3

Abstract

Measurements of parity-violating longitudinal analyzing powers A_z (normalized asymmetries) in polarized proton-proton scattering and in polarized neutron capture on the proton ($n - p \rightarrow d - \gamma$) provide a unique window on the interplay between the weak and strong interactions between and within hadrons. Several new proton-proton parity violation experiments are presently either being performed or are being prepared for execution in the near future: at TRIUMF at 221 MeV and 450 MeV and at COSY (Forschungszentrum Jülich) in the multi-GeV range. A new measurement of the parity-violating γ ray asymmetry with a ten-fold improvement in the accuracy over previous measurements is being developed at LANSCE. These experiments are intended to provide stringent constraints on the set of six effective weak meson-nucleon coupling constants, which characterize the weak interaction between hadrons in the energy domain where meson exchange models provide an appropriate description. The 221 MeV $p - p$ experiment is unique in that it selects a single transition amplitude ($^3P_2 - ^1D_2$) and consequently constrains the weak meson-nucleon coupling constant

*Work supported in part by the Natural Sciences and Engineering Research Council of Canada

†For the E497 Collaboration: J. Birchall, J. Bland, J.D. Bowman, C.A. Davis, P.W. Green, A.A. Hamian, R. Helmer, S. Kadantsev, Y. Kuznetsov, R. Laxdal, L. Lee, C.D.P. Levy, R.E. Mischke, S.A. Page, W.D. Ramsay, S.D. Reitzner, G. Roy, G.M. Stinson, V. Sum, N.A. Titov, W.T.H. van Oers, R-J. Woo, A.N. Zelenski.

h_ρ^{pp}. The $n-p \rightarrow d-\gamma$ experiment is mainly sensitive to the weak pion-nucleon coupling constant f_π. Together with the existing $p-p$ parity violation experimental results one may be able to delineate the various weak meson-nucleon coupling constants. The TRIUMF 221 MeV $p-p$ parity violation experiment will be described in some detail. Other parity violation nucleon-nucleon and nucleon- very-light-nucleus experiments are commented on. The anomalous result obtained at 6 GeV/c on a water target requires that a new multi-GeV $p-p$ parity violation experiment be performed.

(paper submitted to International Journal of Modern Physics E)

1. Introduction

Because flavour changing neutral currents are almost completely suppressed by the G.I.M. mechanism, the study of hadronic neutral currents in nuclear systems provides a unique window on weak neutral currents. Parity violation in nuclear systems is the only flavour conserving process in which hadronic weak neutral currents can be observed. Observations of parity violation in the nucleon-nucleon ($N-N$) systems are complementary to studies of parity violation in electron-proton scattering, the next generation of which is focussing on constraining the possible contributions of strange quarks from the sea to the nucleon form factors and the quest for "new physics".

At low and intermediate-energies, the parity violating weak $N-N$ interaction can be described in terms of a meson exchange model involving a strong interaction vertex and a weak interaction vertex (assuming one-boson exchanges). The strong interaction vertex is generally well understood; it is represented by the conventional meson-exchange parameterization of the nucleon-nucleon interaction. The weak interaction vertex is calculated from the Weinberg-Salam model assuming that the W- and Z-bosons are exchanged between the intermediate mesons (π, ρ, and ω) and constituent quarks of the nucleon. The parity violating interaction can then be described in terms of seven weak meson-nucleon coupling constants. The six weak meson-nucleon coupling constants (f_π, h_ρ^0, h_ρ^1, h_ρ^2, h_ω^0, h_ω^1, with the subscripts indicating the exchanged meson and superscripts indicating isospin changes) have been calculated by Desplanques, Donoghue, and Holstein (DDH)[1], synthesizing the quark model and SU(6) and treating strong interaction effects

in renormalization group theory. The seventh weak meson-nucleon coupling constant $h_\rho^{\prime 1}$ is estimated to be smaller and is often deleted from further consideration. DDH tabulated "best guess values" and "reasonable ranges" for the six weak meson-nucleon coupling constants. Similar calculations have been made by Dubovik and Zenkin (DZ)[2]. Extending the earlier work in the nucleon sector, Feldman, Crawford, Dubach, and Holstein (FCDH)[3] included the weak Δ-nucleon-meson and weak Δ-Δ-meson parity violating vertices for π, ρ, and ω mesons. The latter authors also present "best guess values" and "reasonable ranges" for the six weak meson-nucleon coupling constants. Using the expressions of an earlier paper by Desplanques (D)[4] FCDH present a third set of weak meson-nucleon coupling constants. It is apparent that these coupling constants carry considerable ranges of uncertainty (see Table 1). Taking into account the more recent nuclear parity violation experiments, Desplanques[5] argues for a reduced value and range for the weak meson-nucleon coupling constant f_π. The weak meson-nucleon coupling constants have also been calculated by Kaiser and Meissner (KM)[6] within the framework of a nonlinear chiral effective Lagrangian which includes π, ρ, and ω mesons. In this model f_π is considerably smaller than the "best guess value" of DDH or FCDH (Table 1). Furthermore, a non-zero and non-negligible value for the seventh weak meson-nucleon coupling constant $h_\rho^{\prime 1}$ was found. The parity violating $\pi\Delta N$ vertex plays an important role in elastic and inelastic proton-proton scattering above the pion production threshold. The latter authors[7] find that the isoscalar parity violating $\pi\Delta N$ coupling constant $h^0_{\pi\Delta N}$ vanishes identically, but that the isovector parity violating coupling constant $h^1_{\pi\Delta N}$ has a strength of 2.1×10^{-8} and that the parity violating $\rho\Delta N$ and $\omega\Delta N$ couplings generally cannot be neglected. Meissner and Wiegel[8] find a sizeable enhancement of f_π in the framework of a three flavor Skyrme model compared to previous calculations in two flavor models (f_π ranges from 0.8 to 1.3×10^{-7}). Holstein[9] has re-examined the quark model calculations and has concluded that a small value of f_π cannot be understood unless the current algebra quark mass values are increased by about a factor of two over the original Weinberg values, which tends to produce a similar suppression of theoretical estimates in other areas, e.g., the $\Delta\mathrm{I} = 1/2$ rule. It appears that the theoretical situation regarding f_π is not very well settled. For a recent review see Haeberli and Holstein.[10]

A complete determination of the six weak meson-nucleon coupling

constants demands at least six experimental, linearly independent combinations of the weak meson-nucleon coupling constants. But as of to date there do not exist enough experimental constraints of the required statistical significance. This situation can only be remedied by performing a set of judiciously chosen, precision parity violation experiments.

Impressively precise measurements of the proton-proton parity violating longitudinal analyzing power have been made at 13.6 MeV [A_z = (-0.93 $\pm$ 0.20 $\pm$ 0.05) $\times$ 10^{-7}] at the University of Bonn[11] and at 45 MeV [A_z = (-1.57 $\pm$ 0.23) $\times$ 10^{-7}] at the Paul Scherrer Institute (PSI)[12]. Here A_z is defined as $A_z = (\sigma^+ - \sigma^-)/(\sigma^+ + \sigma^-)$, where σ^+ and σ^- represent the scattering cross sections for polarized incident protons of positive and negative helicity, respectively, integrated over a range of angles determined by the acceptance of the experimental apparatus in question. A non-zero value of A_z implies parity violation due to the non-zero pseudo-scalar observable $\vec{\sigma}.\vec{p}$ with $\vec{\sigma}$ the spin and $\vec{p}$ the momentum of the incident proton. From the PSI measurement at 45 MeV and the $\sqrt{E}$ energy dependence of A_z at lower energies, one can extrapolate A_z at 13.6 MeV to be A_z = (-0.86 $\pm$ 0.13) $\times$ 10^{-7}. There exists thus excellent agreement between the above two lower energy measurements. Both results allow determining a combination of the effective ρ and ω weak meson-nucleon coupling constants $A_z = 0.153 h_\rho^{pp}$ + 0.113h_ω^{pp}, with $h_\rho^{pp} = h_\rho^0 + h_\rho^1 + h_\rho^2/\sqrt{6}$ and $h_\omega^{pp} = h_\omega^0 + h_\omega^1$. It should be noted that a measurement of A_z in $p-p$ scattering is sensitive only to the short range part of the parity violating interaction (parity violating π^0 exchange would simultaneously imply CP violation and is therefore suppressed). However, above the pion production threshold, where intermediate Δ states become important, parity violating charged pion-exchanges play a non-neglegible role. In fact Silbar, Kloet, Kisslinger, and Dubach[13] find that the pion-exchange contribution to A_z has both inelastic and elastic scattering contribution components and is sizable even below the pion production threshold. These authors also argue that strong distortions enhance the magnitude of this contribution.

With the $p-p$ strong interaction phases known from phase shift analyses and given a set of the parity violating mixing angles, one can calculate both the angular and energy dependence of A_z.[14] A partial wave decomposition allows the various contributions to A_z to be separated out. The mixing angles are directly related to the parity violating transition amplitudes ($^1S_0$ - $^3P_0$), ($^3P_2$ - $^1D_2$), ($^1D_2$ - $^3F_2$), ($^3F_4$ - $^1G_4$),

etc. In practise it is almost impossible to measure the angular dependence of the longitudinal analyzing power A_z and consequently one has to resort to measuring an angle-averaged longitudinal analyzing power A_z while at the same time excluding the forward, Coulomb scattering dominated, angular region. A determination of A_z can be accomplished through a scattering measurement, restricted to the low-energy region, or through a transmission (attenuation) measurement at intermediate and higher energies. The energy dependence of the first two parity violating transition amplitudes contributing to A_z is shown in Fig. 1.[15] For energies below 100 MeV essentially only the first parity violating transition amplitude ($^1S_0$ - $^3P_0$) contributes. One notices the increase in importance of the second parity violating transition amplitude for energies above 100 MeV. The theoretical ($^1S_0$ - $^3P_0$) contribution to A_z was normalized to the experimental datum at 45 MeV.[15]. The contribution of the next higher order (third) transition amplitude ($^1D_2$ - $^3F_2$) is negligibly small.

There exists a further $p-p$ parity violation measurement at 800 MeV with $A_z = (2.4\pm1.1)\times10^{-7}$.[16] Interpretation of the latter result in terms of the effective ρ and ω weak meson-nucleon coupling constants is more difficult due to the presence of a large inelasticity (pion production).

Other $N-N$ measurements have dealt with the circular polarization of the gamma-rays in $n-p$ capture[17] or with the longitudinal analyzing power in $n-p$ capture with polarized incident cold neutrons.[18] For low-energy neutrons parity violation in the reaction $n-p \rightarrow d-\gamma$ is almost entirely due to weak pion exchange, as calculated by Adelberger and Haxton[19] and corroborated in an earlier calculation of Desplanques and Missimer.[20] The final result obtained in the last measurement is $A_\gamma = (-1.5 \pm 4.7) \times 10^{-8}$.[18] A new measurement of the parity violating longitudinal analyzing power A_γ is being prepared at the Los Alamos Neutron Science Center (LANSCE), aiming at a ten-fold improvement in accuracy (to a precision of $\pm 0.5 \times 10^{-8}$, which will determine f_π to $\pm 0.4 \times 10^{-7}$).[21] In the experiment, neutrons from the spallation source are moderated by a liquid hydrogen moderator. With the spallation source pulsed, the neutron energy can be determined through time-of-flight measurements. The cold neutrons are polarized by transmission through polarized ^{3}He gas; the neutron spin direction can be subsequently reversed by a RF resonance spin flipper. The neutrons are then guided to a liquid para-hydrogen target which is surrounded by an array of gamma-ray detectors. The parity violating helicity depen-

dence in the inverse reaction, the photodisintegration of the deuteron by circularly polarized gamma-rays, was measured to be $(2.7 \pm 2.8) \times 10^{-6}$ for Bremsstrahlung with an endpoint of 4.1 MeV and $(7.7 \pm 5.3) \times 10^{-6}$ for an endpoint of 3.1 MeV, essentially a null result.[22] A new parity violation experiment, measuring the helicity dependence of the photodisintegration of the deuteron with circularly polarized gamma-rays, may be possible at the HIGS facility of the Triangle Universities Nuclear Laboratory. The very intense gamma-ray beams are obtained from Compton back-scattering using free electron lasers.

The higher flux of neutrons, which will become available from the new cold neutron source at ILL, should make it possible to perform a new generation of $n - p$ parity violation experiments with greatly improved precision. A measurement of the neutron spin rotation in parahydrogen could accomplish the same objective as a measurement of A_γ, in that both observables depend almost entirely on the weak pion-nucleon coupling constant. The expected effect is of the order 10^{-6} rad/m. A University of Washington based group has proposed such an experiment.[23] and expects to achieve a sensitivity of 4σ in 30 days of data taking. A measurement of the parity violating spin rotation of cold neutrons through liquid helium is ongoing at NIST.[24] This rotation, $\Phi(\vec{n}, \alpha)$, is sensitive to the weak pion-nucleon coupling constant, and in conjunction with the result for the $p - \alpha$ longitudinal analyzing power, $A_z(\vec{p}, \alpha)$, obtained at 45 MeV at PSI[25] will determine f_π. A first result of $\Phi(\vec{n}, \alpha)$ equals (8.0 ± 14 [stat] ± 2.2 [syst]) × 10^{-7} rad/m. With $A_z(\vec{p}, \alpha)$ = -(3.34 ± 0.93) × 10^{-7} and the DDH "best values" for $h^0_\rho, h^1_\rho, h^0_\omega, h^1_\omega$ one deduced that $f_\pi = -(1.75 \pm 10.5) \times 10^{-7}$. The accuracies obtained to date in parity violation measurements in the $n - p$ system do not suffice to constrain in a significant way the weak meson-nucleon couplings. For a plot of the constraints on the isoscalar and isovector weak meson-nucleon coupling constants see Fig. 2 (see also Ref. 24).

Following the approach of Adelberger and Haxton[19], one can fit the more significant nuclear parity violation data, using theoretical constraints, by the two parameters f_π and $(h^0_\rho + 0.6h^0_\omega)$. This leaves the experimental value of $f_\pi = (0.28^{+0.89}_{-0.28}) \times 10^{-7}$, as deduced from the circular polarization of the 1.081 MeV γ-rays from ^{18}F (Ref.26), at the border of the deduced range so determined.[10] See Table 1, last two columns.

The definitive non-zero result obtained by Wood et al.[27] in a measurement of the anapole moment of ^{133}Cs has been analyzed by Flambaum and Murray[28] to extract a value for f_π. The resulting value of $f_\pi = (9.5 \pm 2.1[\text{exp.}] \pm 3.5[\text{theor.}]) \times 10^{-7}$ is a factor of two larger than the DDH "best guess value" (see Table 1) and a factor of seven larger than the upper limit set by the ^{18}F results. But Wilburn and Bowman[29] argue that the anapole moment is sensitive to a combination of f_π and h^0_ρ ($f_\pi + 0.69h^0_\rho$) and therefore to deduce f_π one must know h^0_ρ, which still carries a considerable range of uncertainty. Furthermore, the result from ^{133}Cs is inconsistent with an earlier null measurement of the anapole moment of ^{205}Tl.[30] One can then ask the question if there exists a dependence of the weak meson-nucleon coupling constants on the nuclear medium.

Fig.1 shows that there exists a unique feature at an energy of about 230 MeV: the ($^1S_0$ - $^3P_0$) transition amplitude contribution integrates to zero. This reflects a change in sign of both the $^1S_0$ and $^3P_0$ strong interaction phases near 230 MeV and is completely independent of the weak meson-nucleon coupling constants. The absolute scale and sign of the ordinate in Fig. 1, (A_z), are determined by the weak interaction. Neglecting a small contribution ($\approx$5%) from the ($^1D_2$ - $^3F_2$) transition amplitude, a measurement of A_z near 230 MeV constitutes a measurement of the contribution of the ($^3P_2$ - $^1D_2$) transition amplitude. Simonius[31] has shown that the ($^3P_2$ - $^1D_2$) transition amplitude depends only weakly on ω-exchange (to an extent determined by the choice of the strong vector meson-nucleon coupling constants from various $N-N$ potential models), whereas ρ-exchange and ω-exchange contribute to the ($^1S_0$ - $^3P_0$) transition amplitude with equal weight. Consequently, a measurement of A_z at an energy of 230 MeV presents a determination of h^{pp}_ρ. The energy dependence of the real parts of the $p-p$ phase shifts predicts that, neglecting inelasticity, the ($^1D_2$ - $^3F_2$) transition amplitude changes sign at about 650 MeV, and that the ($^3P_2$ - $^1D_2$) transition amplitude changes sign at about 950 MeV. Precision measurements of A_z at both 230 MeV and 650 MeV could provide another determination of both h^{pp}_ρ and h^{pp}_ω (in addition to a combination of the low energy measurements with a measurement at 230 MeV).

Various theoretical predictions of the $p-p$ longitudinal analyzing power A_z, based on meson-exchange models, have been reported: at 230 MeV the values of A_z are $= +0.7 \times 10^{-7}$ (Ref. 32), $+0.6 \times 10^{-7}$ (Ref. 15), and $+0.4 \times 10^{-7}$ (Ref. 33). Extensions to the one-boson

exchange model have been made to include $\pi - \pi$ and $\pi - \rho$ exchanges via $N - \Delta$ and $\Delta - \Delta$ intermediate states to which the ($^3P_2$ - $^1D_2$) transition amplitude is particularly sensitive.[13,32] For instance, Iqbal and Niskanen[32] find that the Δ isobar contribution at 230 MeV (which is dependent on f_π) may be as large as the ρ-exchange contribution, enhancing the value of A_z by a factor of two. What is required is a self-consistent theoretical calculation of A_z, avoiding possible double counting and taking into account that the value of f_π is constrained by experiment to be rather small. The latter assumes that the discrepancy which has arisen by the measurement of a large anapole moment of ^{133}Cs has been resolved. It is to be noted that the prediction of A_z by Nessi-Tedaldi and Simonius[15] had been normalized to the experimental datum at 45 MeV as remarked above. Driscoll and Miller[33] predict a rather small value for A_z; their theoretical curve does not agree very well with the two low-energy data. Scaling to the low-energy experimental data at 13.6 and 45 MeV, would give an even smaller value for A_z at 230 MeV indeed. Considering all of the above, a measurement of A_z at 230 MeV to an accuracy of $\pm 2 \times 10^{-8}$ would provide a most important determination of parity violation in $p - p$ scattering. Following the formalism of Simonius[15] and taking into account the finite geometry of the TRIUMF $p - p$ parity violation experiment described below one can show that A_z(221 MeV) = -0.0296 $\times$ h_ρ^{pp}.

2. The TRIUMF 221.3 MeV $p - p$ Parity Violation Experiment (see Fig. 3)

In the current TRIUMF experiment a 200 nA proton beam with a polarization of 0.80 is incident on the 0.40 m long LH_2 target, after extraction from the optically pumped polarized ion source (OPPIS), passing a Wien filter in the injection line, acceleration through the cyclotron to an energy of 221.3 MeV, and multiturn extraction of the H^- polarized ions. The incident energy was chosen to correspond to integration to zero of the contribution of the ($^1S_0$ - $^3P_0$) transition amplitude over the finite acceptance of the parity violation measuring apparatus. A combination of solenoid-dipole-solenoid-dipole magnets on the external beam line provides a longitudinally polarized beam with either positive or negative helicity. The longitudinal analyzing power A_z follows from the helicity dependence of the $p-p$ total cross section as determined in precise measurements of the normalized transmission asymmetry through

the 0.40 m long LH_2 target: $A_z = -(1/P)(T/S)(T^+ - T^-)/(T^+ + T^-)$, where P is the incident beam longitudinal polarization, $T = 1 - S$ is the average transmission through the target, and the + and − signs indicate the helicity state.

There are many other effects that can cause such a helicity correlated change in transmission. Very strict constraints are imposed on the incident longitudinally polarized beam in terms of intensity, transverse x (horizontal) and y (vertical) beam position and direction, beam width (given by σ_x and σ_y), longitudinal polarization (P_z), transverse polarization (given by P_y and P_x), first moments of the transverse polarization (given by $< xP_y >$ and $< yP_x >$), and energy, together with deviations of the transmission measuring apparatus from spatial symmetry. Helicity correlated modulations in the beam parameters originate at OPPIS, but can be amplified by the beam transport through the injection beam line, the cyclotron accelerator and the extraction beam line. Residual systematic errors, arising from the imperfections of the incident beam and the response of the transmission measuring apparatus, are individually not to exceed one tenth of the expected value of A_z (or 6×10^{-9}). Particular troublesome are the first moments of the residual transverse polarization (so called "circulating" polarization profiles), as well as energy changes. In addition to the strict constraints imposed on the incident beam parameters and on the quality of the measuring apparatus, the approach which is being followed is to further measure the sensitivity or response to residual imperfections, to monitor these imperfections during data taking, and to make corrections where necessary. Random changes of the incident beam parameters cause a dilution of the effect to be measured and therefore longer data taking times in order to arrive at the desired statistical error.

Helicity changes are implemented through shifts in the linearly polarized laser light frequency (a frequency change of 94 GHz at a magnetic field of 2.5 T), minimizing helicity correlated changes in the accelerated beam parameters. The optimum beam current at the parity violation measuring apparatus is 200 nA; to achieve very small helicity correlated modulations, most of the OPPIS intensity is sacrificed for beam quality. As an example, the RF bunchers in the injection beam line, used to enhance the cyclotron transmission by a factor of four, also increase the sensitivity to energy modulations by more than two orders of magnitude and therefore cannot be used in the parity violation

experiment. A high brightness OPPIS was developed for the parity violation experiment; simultaneous high-current OPPIS development[35] for high-energy accelerators has contributed greatly to the parity violation experiment. The Faraday effect provides a means to monitor and control on-line the polarization of the Rubidium vapour (which produces electron polarized $\vec{H}^0$ through charge exchange) by using a probe laser. The polarization of the linearly polarized laser light is rotated by an angle proportional to the Rubidium vapour polarization. The polarizations of the Rubidium vapour in the two helicity states are maintained to be the same within 0.005 close to 1.00. The Faraday rotation measurement also provides confirmation of the helicity state at OPPIS.

To aid in tuning the extracted polarized proton beam, various retractable horizontal and vertical wire chambers are placed along the beam line. Following the second dipole magnet, where the polarization direction has both a longitudinal and a horizontal sideways component, a four branch polarimeter measures the transverse polarization components, while a beam energy monitor measures the relative energy of the proton beam with a precision of $\pm$ 20 keV during a one hour data taking run. Measurements are made several times each data taking period. The absolute energy has to agree within a few MeV with the energy for which the ($^1S_0$ - $^3P_0$) transition contribution integrates to zero, taking into account the finite geometry of the transmission measuring apparatus; but note that any changes in energy greater than 40 keV will introduce transverse polarization components at the transmission measuring apparatus in excess of 0.001 for the canonical setting of all beam transport magnetic elements. All beam transport magnetic elements have their excitations monitored on a continuous basis (superconducting solenoids - currents; dipole magnets using NMR probes; quadrupole magnets using Hall probes).

Figure 4 gives a three dimensional view of the downstream part of the experimental setup. The longitudinally polarized beam, incident from the lower right, passes first a series of diagnostic devices - a set of three beam intensity profile monitors (IPMs), and a pair of transverse polarization profile monitors (PPMs) - before reaching the LH_2 target which is preceded and followed by transverse electric field ionization chambers (TRICs) to measure the beam current. Note the position of the third IPM.

Ideally the beam transport is to produce an achromatic waist downstream of the LH_2 target halfway into the second transverse electric field ionization chamber (TRIC-2). The beam is converging downstream of the last quadrupole magnet triplet; its dimensions at the location of the first two IPMs are characterized by ($\sigma_x = \sigma_y$ and the x and θ parameters decoupled from the y and ϕ parameters). Helicity changes can also be accomplished by reversing the currents of the two super-conducting solenoids. The rotation of phase space introduced by the super-conducting solenoids is negated by rotation around the beam line axis of various sets of quadrupole magnets. Consequently the reversal of the solenoid currents requires simultaneous reversal of the quadrupole rotation angles. Empirical beam line tunes were developed which are very similar for the 'normal' and 'reversed' solenoid excitation settings. These empirical tunes deviated in certain aspects from the specified, calculated, beam line tunes.

Helicity correlated current modulations, expressed as $\Delta I/I = (I^+ - I^-)/(I^+ + I^-)$, introduce a systematic error ΔA_z through non-linearity of the TRICs and associated electronics. The parity detection apparatus attains minimal sensitivity to these current modulations by precision analog subtraction of the current signals of the two TRICs. Controlled helicity correlated current modulations are needed for tuning the precision subtractor circuitry for minimal sensitivity. These control measurements are provided by an auxiliary argon-ion laser beam which co-propagates with the H^- beam along the 30 m long horizontal section of the injection beam line (as shown in Fig. 3), neutralizing through photodetachment a fraction of the H^- ions along its path. The photodetachment laser is interrupted synchronously with the parity spin sequence, so that the beam current in every second spin 'off' data taking cycle is modulated at the 0.1% level, giving the desired control measurements. Improvements to the stabilization of the Electron Cyclotron Resonance (ECR) primary proton source, the Rubidium vapour thickness in the polarizer cell, OPPIS high voltage levels, the injection beam line elements (in particular the Wien filter), and the cyclotron accelerator have led to a reduction in the width of ΔI/I to about the required 1×10^{-5}. Table 2 presents a comparison of calculated and measured sensitivities to systematic errors and the precision required in measuring the various parameters.

The IPMs[36], which are based on secondary electron emission from thin, 3 μm thick nickel foil strips placed between 8 μm aluminium

high voltage foils, measure the beam intensity profile with harps of 31 strips (1.5 mm wide, separated 2.00 mm center to center) in both the vertical (x-profile) and horizontal (y-profile) directions. (Fig. 5) The third IPM placed just in front of the LH_2 target has 10 μm thick nickel foil strips (2.5 mm wide by 3.00 mm center to center). The harp signals are individually amplified and digitized to provide the beam intensity profiles in x and y, from which the beam positions are derived. Analog beam centroid evaluators (BCEs) in turn determine the beam intensity profile centroids at two locations through appropriate integration of the discrete distributions; a corresponding normalized error signal is used to drive feedback loops to a pair of x and y fast, ferrite-cored steering magnets. This allows the beam intensity profile centroids to be kept fixed within 1 μm with an offset less than 50 μm from the 'neutral' axis in both x and y during a one hour data taking run. The beam intensity profile widths maintained during data taking are: IPM-1 σ_x = σ_y = 5 mm; IPM-2 = 4 mm; IPM-3 = 6 mm. Typical values for the modulations in position and width in a one hour data taking run are Δx, Δy $< (0.5 \pm 0.3)$ μm and $\Delta\sigma_x$, $\Delta\sigma_y < (1.0 \pm 0.6)$ μm. Sensitivities to helicity correlated position and size modulations are determined with enhanced modulations introduced using the fast, ferrite-cored magnets synchronized to the helicity sequence of the experiment to allow for off-line corrections. The advantage of the BCE based position stabilization system over the earlier median intensity based position stabilization system (which used the amplified signals from split foil monitors) is a reduction in sensitivity to shape fluctuations in the beam intensity profiles.

The PPMs are based on $p - p$ scattering using CH_2 targets. Scattered protons are detected in a forward arm at 17.5° with respect to the incident beam direction with a pair of scintillation counters. The solid angle defining scintillator is rotated around an axis perpendicular to the scattering plane to compensate for changes in solid angle and differential cross section, when the CH_2 target blade moves through the beam (see Fig. 6). Coincident recoil protons are detected in a backward arm at 70.6° with respect to the incident beam direction with a recoil scintillation counter; a second scintillation counter acts as a veto for higher energy protons from ^{12}C(p,p)X. Each PPM contains detector assemblies for 'left' scattered protons, 'right' scattered protons, 'down' scattered protons, and 'up' scattered protons. The targets consist of CH_2 blades, 1.6 mm wide by 5.0 mm thick along the incident beam

direction. The blades move through the beam on a circle of 0.215 m at a frequency of 5 Hz. Each PPM has four blades; two which scan the polarization profile in the horizontal direction and allow for determining the quantity $(L-R)/(L+R)$ and therefore P_y as a function of x for each of the two helicity states, and two which scan the polarization profile in the vertical direction and allow for determining the quantity $(D-U)/(D+U)$ and therefore P_x as a function of y for each of the two helicity states. Residual transverse polarizations (which change sign with helicity reversals) can cause a false A_z via the parity allowed transverse analyzing power, which produces asymmetric scattering in the LH_2 target. The sensitivities to transverse polarizations are dependent on the incident beam position and on the geometry of the parity violation measuring apparatus. Proper beam tuning greatly reduces (by a factor of approximately 20) the transverse polarizations at the LH_2 target compared to those at injection of the cyclotron. Both the sensitivities and the 'neutral axis' are determined by introducing enhanced transverse polarizations P_x and P_y. Non-zero first moments of the transverse polarizations, $< xP_y >$ and $< yP_x >$, can arise from an inhomogeneous polarization distribution of the cyclotron beam at the stripper foil location, and from spin precession in the magnetic field gradients at the entrance and exit of the solenoids, dipole magnets, and quadrupole magnets. The latter combined have been estimated to contribute less than 10 μm to the transverse polarization moments. The sensitivity to intrinsic first moments is determined by deducing the correlations between apparent A_z and the $< xP_y >$ and $< yP_x >$ as measured by the PPMs. The moments of transverse polarization exhibit a random variation from run to run and reach values as high as 30 μm as measured in one hour data taking runs. In a drift space first moments vary linearly with position along the beam line, permitting the adjustments of the beam transport parameters such that the first moments pass through zero at a point which minimizes their effect. Reducing the first moments of transverse polarization was one of the more challenging aspects of the experiment; it required frequent retuning of OPPIS, the cyclotron, and beam transport systems. With measured sensitivities to $< xP_y >$ and $< yP_x >$ of $+5 \times 10^{-5}$ mm^{-1} and -8×10^{-5} mm^{-1}, respectively, one needs to measure these to a precision of 12×10^{-5} mm and 8×10^{-5} mm, respectively, over the course of the experiment in order that their possible individual contribution to the error in A_z is less than 6×10^{-9}.

With two PPMs, each with four blades, the spin flip or helicity flip rate becomes 40 Hz, i.e., in one cycle all eight blades of the two synchronized PPMs (four blades of PPM-1 and four blades of PPM-2) will pass once through the beam. The master clock for sequencing the entire experiment, including helicity changes, is derived from the PPMs shaft encoders. In order to suppress up to second order other than helicity correlated effects stemming from changes in the incident polarized beam parameters, a cycle consists of the following sequence of helicity states: $+--+-++-$, lasting 200 ms. Eight cycles are repeated, with the first helicity state chosen so as to form an eight by eight symmetric matrix of helicity states (designated a super-cycle). After three of such super-cycles, the pumping laser light is blocked by a shutter during one super-cycle for control measurements. In every other super-cycle used for control measurements, the sensitivity to helicity correlated changes in the incident beam intensity is measured. Of each helicity state of 25 ms duration, a little more than 1 ms is reserved for the polarization to stabilize following a helicity change, the next 6.4 ms is used for the measurement of the transverse polarization (one of the CH_2 blades whisking through the incident beam), and precisely 1/60 sec is used for the actual parity violation measurement (determining the helicity dependent transmission). A small phase slip is introduced so that the master clock and the line frequency are again precisely in phase after 18 minutes.

The LH_2 target (Fig. 7) has a flask of 0.10 m diameter and a length of 0.40 m. Special precautions have been taken to make the end windows of the target flask optically flat and parallel. Maximum heat load of the target is 25 W with operation at approximately 5 W. By circulating the liquid hydrogen rapidly (5 l/s), density gradients are minimized. The target flask is remotely movable within $\pm$ 5 mm in two orthogonal directions at both ends to position it on the 'neutral axis'. The total scattering probability at 221.3 MeV by the 0.40 m long LH_2 is close to 4%. The target flask length is limited by multiple Coulomb scattering considerations; the various entrance and exit windows of the LH_2 target (and all other energy degrading foils in the beam) are kept to the minimally allowable number and thickness.

The main detectors are two transverse electric field ionization chambers, producing current signals due to direct ionization of the ultra-high purity hydrogen gas by the beam. Field shaping electrodes plus guard rings ensure a 0.15 m wide by 0.15 m high by 0.60 m long sense region

between the parallel electrodes (negatively charged anode and signal plate), with the electric field lines all parallel and perpendicular to the electrodes. The TRICS have been designed for operation at -35 kV at one atmosphere; in practice they are operated at a pressure of about 150 torr and a high voltage of -8 kV. The entrance and exit windows are located at approximately 0.9 m from the center of the TRICs to range out spallation products from proton interactions with the stainless windows. (see Fig. 8 The design of the TRICs incorporated considerations of noise due to δ-ray production and due to recombination.

The proton beam energy in the downstream TRIC is on average 27 MeV lower than in the upstream TRIC due to the difference in the energy loss in the LH_2 target. Helicity correlated energy modulations will cause a false A_z due to the energy dependence of the energy loss in the hydrogen gas of the TRICs. The sensitivity to coherent energy modulations was determined using a RF accelerating cavity placed upstream of IPM-1 in the beam line. The RF cavity could produce coherent energy modulations with an amplitude of 600 eV in the 221.3 MeV proton beam. The measured sensitivity of $(2.9 \pm 0.3) \times 10^{-8}$ eV^{-1} agrees very well with the prediction obtained in Monte Carlo simulations of the experiment of 2.8×10^{-8} eV^{-1} and places a very stringent constraint on the maximally allowable helicity correlated energy modulation of the incident proton beam. Coherent energy modulations of the extracted beam are caused by coherent modulations of the radial intensity distribution at the cyclotron stripping foil; this converts position modulations of the injected beam to energy modulations of the extracted beam. The conversion factor has been estimated to be dE/dx_{injected} =100 eV/μm which is in agreement with direct measurements made by applying large position modulations of the injected beam using electrostatic steering plates. One source of the helicity correlated position modulations of the injected beam is helicity correlated energy modulations at OPPIS, which are converted to position modulations when the beam passes electrostatic steering plates on its way to injection into the cyclotron. This process amplifies the primary coherent energy modulations at OPPIS by a factor of approximately 100, as determined in an auxiliary measurement using a magnetic spectrometer. The sensitivity of A_z to helicity correlated energy modulations at the ion source OPPIS was measured by applying a square wave voltage of 0.5 V amplitude to the sodium ionizer cell in OPPIS. A sensitivity of 0.4×10^{-8} per meV of coherent energy modulation at OPPIS was

measured in agreement with the conversion factor measurement. Consequently, coherent energy modulations at OPPIS are not to exceed about 1 meV. The other source of helicity correlated position modulations of the injected beam are helicity correlated position modulations at OPPIS; the measured sensitivity of A_z is approximately 0.1×10^{-8} per nm of helicity correlated beam position modulation at OPPIS. Consequently, coherent position modulations at OPPIS are not to exceed about 4 nm. Coherent energy and position modulations were monitored on a regular basis at OPPIS using a pair of electrostatic steering plates as a beam analyzer and an intensity profile monitor with 16 foil strips to measure the beam position downstream of the steering plates. Measuring on both sides of the OPPIS beam axis allowed for both energy and position modulations to be determined. The precisions obtained after 20 minutes are $\pm$ 2 nm in position and 0.2 meV in energy. But helicity correlated energy modulations cannot be directly measured at the parity violation measuring apparatus. Therefore, an appropriate linear combination of the data taken with all possible helicity combinations and spin precessions is being used to remove any false A_z due to helicity correlated energy modulations.

To date a series of data taking runs have taken place. Of these the second and fourth data taking runs have been analyzed. The preliminary result is shown in Fig. 9 and compared with the theoretical prediction of Driscoll and Miller[33]. The theoretical prediction of Driscoll and Miller is based on the Bonn potential to represent the strong interactions together with the weak meson-nucleon coupling constants as given by Desplanques, Donoghue, and Holstein[1]. It treats Coulomb effects and relativistic distortions, but inelastic effects are treated in an indirect manner. Even though the Driscoll and Miller theoretical prediction overestimates the size of A_z at the lower energies (correctible through adjustment of the weak ρ- and ω-nucleon coupling constants), it exhibits the expected energy behavior. Figure 10 compares various theoretical predictions with the low energy $p - p$ parity violation data. The theoretical prediction of Grach and Shmatikov[37] is based on a quark model which emphasizes the second transition ${}^3P_2$-${}^1D_2$ contribution leading to a rather different energy dependence. The theoretical predicton of Iqbal and Niskanen[32] has a Δ isobar contribution included. The theoretical prediction of Driscoll and Meissner is based on a self consistent calculation, with both weak and strong vertex functions obtained with a chiral soliton model. Note the small value of A_z predicted

at 221 MeV. Figure 11 gives the constraints placed on the weak meson-nucleon coupling constants by the $p-p$ parity violation experiments. It is anticipated that continued data taking and data analysis will give the 221 MeV experimental result uncertainties less than 2×10^{-8} in statistics and in systematics.

3. Proton-proton Parity Violation Measurements at Higher Energies

A further $p-p$ parity violation experiment is in preparation at TRIUMF at an energy of 450 MeV.[38] With an inelasticity of at most 10% of the total cross section, the expected impact on the deduction of the combination of weak meson-nucleon coupling constants h_ρ^{pp} and h_ω^{pp} is considerably less than the aimed-for experimental errors of 2×10^{-8} in statistics and 2×10^{-8} in systematics. The measurement can be made with minimal changes to the apparatus of the present TRIUMF $p-p$ parity violation experiment, except for modifications to the PPMs to allow higher count rates. The combination of measurements at 221 MeV and 450 MeV would give an independent determination of the weak meson-nucleon coupling constants h_ρ^{pp} and h_ω^{pp}.

Measurements of A_z in $p-p$ scattering have also been proposed at COSY of the Forschungszentrum Jülich as a fixed target experiment near 230 MeV and at a higher energy as a cooler ring experiment.[39] The choice of the latter energy (or better an energy close to the maximum energy of COSY) is in part motivated by the earlier 5.13 GeV measurement of A_z (on a water target) at the ZGS of Argonne National Laboratory, which resulted in $A_z = (26.5 \pm 6.0 \pm 3.6) \times 10^{-7}$.[40] This result is an order of magnitude larger than what is expected using conventional scaling arguments. It must be remarked that various re-evaluations of the experiment have not come across any flaw (in the way the experiment was conducted) that could have led to such a large false A_z. It has also been pointed out that when Glauber shadowing is taken into account, the $p-p$ parity violating A_z increases by as much as 40%.[41] Figure 12 shows the energy dependence of A_z; note the logarithmic scale used for the abscissa.

The theoretical curve[42] that matches the experimental data at 800 MeV and at 5.13 GeV has been normalized to the 5.13 GeV datum. This calculation is based on a diquark model introducing a parity violating component in the nucleon wave function. The authors find an important role for diagrams in which the weak interactions between the

members of a vector diquark in the polarized proton is accompanied by the strong interaction between that diquark and a quark of the other nucleon. The theoretical curve exhibits a steep increase for A_z with increasing energy. It predicts a value for A_z at 20 GeV of the order 10^{-5}. Note that a 200 GeV experiment has placed an upper limit (95% C.L.) on the $p-p$ longitudinal analyzing power A_z of 5.7×10^{-5} (Ref. 43). The theoretical interpretation[42] of the unexpectedly large result for A_z at 5.13 GeV has created a great deal of controversy[44]. Many of the earlier theoretical predictions for A_z give values of the order of 10^{-7} at 5.13 GeV; see for instance Ref. 45. Clearly, the 5.13 GeV result presents a great challenge both in obtaining its confirmation through a new 5 GeV experiment and in obtaining a self-consistent theoretical explanation.

If confirmed experimentally, the need for a further experiment at an energy of tens of GeV becomes well established indeed. Such a second higher energy measurement of parity violation in $p-p$ scattering could be made at the AGS of Brookhaven National Laboratory[46] or at the proposed Japanese Hadron Facility. It has been pointed out that a storage ring/internal target environment would allow for innovative methods in performing such an experiment, quite different from the methods used in all previous $p-p$ and proton-nucleus parity violation experiments[47]. A schematic illustration of a possible $p-p$ parity violation experiment in a storage ring with an internal target is shown in Fig. 13. The polygonal ring has a twelvefold symmetry. The Siberian snake of the "first kind" precesses the spin direction of the polarized protons of the beam by 180 degrees about the longitudinal axis. When energized the Siberian snake causes the stable spin orientation in each straight section of the ring to be horizontal, rather than vertical. Choosing the appropriate beam energy, corresponding to half integer spin tune of $G\gamma = 7.5$, or 13.5, etc. (where G is the anomalous magnetic moment of the proton and γ is the standard relativistic factor) one arrives at a stable spin direction for the various straight sections of the ring as indicated (beam energies of 2.99 GeV, 6.13 GeV, etc.). The attenuation of the stored beam has to be dominated by the nuclear scattering and not by Coulomb scattering. Consequently an energy of a few GeV may be too low for a storage ring parity violation experiment. One should note that the stable spin direction for any bombarding energy is longitudinal in the straight section located diametrically opposite the Siberian snake (see Fig. 13). Consequently,

this is the location to perform the transmission experiment with an internal gaseous high purity hydrogen target. The unwanted transverse polarization components of the beam at this location reverse sign upon each successive passage of the Siberian snake and are therefore very effectively cancelled. As stated above for the 221 MeV TRIUMF $p-p$ parity violation experiment, these transverse polarization components and their first moments can cause significant systematic errors in external, fixed target experiments. The spin direction of the stored beam can be flipped rapidly by an 'adiabatic fast passage' technique using an 'RF field' also indicated in Fig. 13 and independently at a lower rate by helicity reversal at the polarized ion source between successive beam injection into the ring[47]. The attenuation experiment consists of determining the helicity dependence of the stored beam lifetime by a current transducer. The resolution of the current transducer is one of the determining factors for the precision attainable in a storage ring experiment. Such current monitors are being developed[48]. The use of a windowless gaseous pure hydrogen target as well as the cancellation of the extraneous transverse polarization components are the distinct advantages of the stored beam/internal target environment. The ring will also act as a magnetic spectrometer, so that the experiment becomes insensitive to a false parity violation signal caused by weak decays of the hyperons produced in $p-p$ interactions. Of concern are, however, the interactions of the stored beam with the residual gas in other sections of the ring, where the polarization direction of the beam is not longitudinal, or the presence of beam halo interacting with the ring structure, as well as helicity correlated changes in beam emittance in successive injection cycles or upon 'RF field' induced spin flips. Clearly, a thorough evaluation through simulations is needed to underpin the asserted advantages of the storage ring/internal target environment for any $p-p$ parity violation experiment.

Information about the flavor non-conserving hadronic weak interaction stems from non-mesonic decays of hypernuclei. Increasingly for heavier and heavier hypernuclei, the Λ inside the nuclear medium does not decay through the (by the Pauli principle blocked) mesonic channel, but through the $\Delta\mathrm{S}=1$ non-mesonic channel, $\Lambda-N\rightarrow N-N$. Less theoretical encumbrance is provided by studying the inverse reaction $p-n\rightarrow p-\Lambda$ (threshold energy 368.5 MeV). However, the expected small cross section of less than 10^{-13} times the $p-n$ elastic scattering cross section poses a great experimental challenge, which has not yet

been met. Most promising, possibly, appears a study of quasi-free Λ production in $d-p \rightarrow p-p-\Lambda$ below the threshold for associated production $d-p \rightarrow p-n-\Lambda-K^+$. Detection of the two protons allows for a determination of the missing mass (selecting the mass of the Λ permits suppression of $p-p-n$ events), while the observation of the decay of the Λ into $p-\pi^-$ excludes strong interaction π^- production (like $p-p-p-\pi^-$ events). Delayed Λ decay occurs on average 50 mm downstream of the Λ production vertex. Complete reconstruction of the $\Lambda \rightarrow p-\pi^-$ decay presents a highly desirable additional kinematical constraint on the weak Λ production. A study of the reaction $d-p \rightarrow p-p-\Lambda$ has been proposed at COSY[49]; the very small cross section poses great demands on the quality and intensity of the longitudinally polarized beam and on the detection system with second and possibly third level fast triggers. A study of the reaction $p-n \rightarrow p-\Lambda$ on a nuclear target has been proposed at RCNP[50]. Again the proposed detection system is quite complex and relies on detection of the Λ decay products in a region shielded from direct view by the target. Recent theoretical predictions of the cross sections and analyzing powers and their energy dependence are given in Ref. 51,52. The observables are found to be rather sensitive to the opening of the Σ^0 production channel (at 540.0 MeV for $p-n \rightarrow p-\Sigma^0$).

4. Conclusions

Several new $N-N$ parity violation experiments are currently being executed; these allow one to anticipate a determination in the near future of the weak meson-nucleon coupling constants and a resolution of the present uncertainty about the weak pion-nucleon coupling constant. The TRIUMF $p-p$ parity violation experiment has produced a first result and is in the final stages of data taking. A measurement of the parity violating neutron spin rotation in helium is ongoing at NIST, while a measurement of the parity violating asymmetry in the capture of longitudinally polarized neutrons by hydrogen has started at LANSCE.

References

[1] B. Desplanques, J.F. Donoghue, and B.R. Holstein, Ann. Phys. (N.Y.) 124, 449 (1980).
[2] V.M. Dubovik and S.V. Zenkin, Ann. Phys. (N.Y.) 172, 100 (1986).
[3] G.B. Feldman, G.A. Crawford, J. Dubach, and B.R. Holstein, Phys. Rev. C43, 863 (1991).
[4] B. Desplanques, Nucl. Phys. A335, 147 (1980).
[5] B. Desplanques, in Parity Violation and Time Reversal Invariance, ed. N. Auerbach and J.D. Bowman (World Scientific, Singapore, 1996), p.98.
[6] N. Kaiser and U-G. Meissner, Nucl. Phys. A499, 699 (1989).
[7] U-G. Meissner and N. Kaiser, Nucl. Phys. A510, 759 (1990).
[8] U-G. Meissner and H. Wiegel, Phys. Lett. B447, 1 (1999).
[9] B.R. Holstein, in Proceedings of the Workshop on Spin and Symmetries, ed. W.D. Ramsay and W.T.H. van Oers, Can. J. Phys. 66, 510 (1988).
[10] W. Haeberli and B.R. Holstein, in Symmetries and Fundamental Interactions in Nuclei, ed. W.C. Haxton and E.M. Henley (World Scientific, Singapore, 1995), p.17.
[11] P.D. Eversheim, *et al.*, Phys. Lett. B256, 11 (1991); P.D. Eversheim, private communication (1994).
[12] S. Kistryn, *et al.*, Phys. Rev. Lett. 58, 1616 (1987).
[13] R.R. Silbar, W.M. Kloet, L.S. Kisslinger, and J. Dubach, Phys. Rev. C40, 2218 (1989).
[14] J. Birchall, G. Roy, and W.T.H. van Oers, Phys. Rev. D37, 1769 (1988).
[15] M. Simonius, in Proceedings of the Symposium/Workshop on Spin and Symmetries, ed. W.D. Ramsay and W.T.H. van Oers, Can. J. Phys. 66, 245 (1988); F. Nessi-Tedaldi and M. Simonius, Phys. Lett. B215, 159 (1988).
[16] V. Yuan, *et al.*, Phys. Rev. Lett. 57, 1860 (1986).
[17] V.A. Knyazkov, *et al.*, Nucl. Phys. A417, 209 (1984).
[18] J.F. Cavagnac, B. Vignon, and R. Wilson, Phys. Lett. 67B, 148 (1977); J. Alberi, *et al.*, in Proceedings of the Symposium/Workshop on Spin and Symmetries, ed. W.D. Ramsay and W.T.H. van Oers, Can. J. Phys. 66, 542 (1988).
[19] E.G. Adelberger and W.C. Haxton, Ann. Rev. Nucl. Part. Sci. 35, 501 (1985).
[20] B. Desplanques and J. Missimer, Nucl. Phys. A300, 286 (1978).
[21] J.D. Bowman, spokesman, LANSCE proposal (1998).
[22] E.D. Earle *et al.*, in Proceedings of the Symposium/Workshop on Spin and Symmetries, ed. W.D. Ramsay and W.T.H. van Oers, Can. J. Phys. 66, 534 (1988).
[23] E.G. Adelberger, in Proceedings of the Symposium/Workshop on Parity Violation in Hadronic Systems, ed. J. Birchall and W.T.H. van Oers (TRIUMF Report 87-3, 1987), p.50.
[24] D.M. Markoff, Ph.D. thesis, University of Washington (1997), unpublished.
[25] J. Lang *et al.*, Phys. Rev. C34, 1545 (1986).
[26] S.A. Page *et al.*, Phys. Rev. C35, 1119 (1987); M. Bini *et al.*, Phys. Rev. C38, 1195 (1988).
[27] C.S. Wood *et al.*, Science 275, 1759 (1997).
[28] V.V. Flambaum and D.W. Murray, Phys. Rev. C56, 1641 (1997).
[29] W.S. Wilburn and J.D. Bowman, Phys. Rev. C57, 3425 (1998).
[30] P.A. Vetter *et al.*, Phys. Rev. Lett. 74, 2658 (1995).
[31] M. Simonius, in Interaction Studies in Nuclei, ed. H. Jochim and B. Ziegler (North Holland, Amsterdam, 1975) p.3; in High Energy Physics with Polarized Beams and Targets, ed. C. Joseph and J. Soffer (Birkhauser Verlag, Basel, 1981), p.355.
[32] M.J. Iqbal and J. Niskanen, Phys. Rev. C42, 1872 (1990); private communication (1994).
[33] D.E. Driscoll and G.A. Miller, Phys. Rev. C39, 1951 (1989); ibid C40, 2159 (1989).

[34] D.E. Driscoll and U-G. Meissner, Phys. Rev. C41, 1303 (1990).
[35] A.N. Zelenski, *et al.*, in Polarized Gas Targets and Polarized Beams (1997), ed. R.J. Holt and M.A. Miller, AIP Conference Proceedings 421, p.372.
[36] A.R. Berdoz *et al.*, Nucl. Instr. and Meth. A307, 26 (1991).
[37] I. Grach and M. Shmatikov, Phys. Lett B316, 467 (1993).
[38] TRIUMF Proposal E761, J. Birchall, S.A. Page, and W.T.H. van Oers, spokespersons.
[39] P.D. Eversheim *et al.*, in High Energy Spin Physics, ed. K-H. Althoff and W. Meyer (Springer Verlag, Berlin, 1991), p.573.
[40] N. Lockyer *et al.*, Phys. Rev. D30, 860 (1984).
[41] L.L. Frankfurt and M.I. Strikman, Phys. Rev. D33, 293 (1986).
[42] T. Goldman and D. Preston, Phys. Lett. 168B, 415 (1986).
[43] D.P. Grosnick, *et al.*, Phys. Rev. D55, 1159 (1997).
[44] M. Simonius and L. Unger, Phys. Lett. B198, 547 (1987); T. Goldman, in Future Directions in Particle and Nuclear Physics at Multi-GeV Hadron Facilities, ed. D.F. Geesaman (Brookhaven National Laboratory Report BNL-52389, 1993), p.140; M. Simonius, ibid., p.147.
[45] T. Oka, Prog. Theor. Phys. 66, 977 (1981); A. Barroso and D. Tadic, Nucl. Phys. A364, 194 (1981).
[46] T. Roser, Workshop on Parity Violations in Hadronic and Nuclear Systems, INT (University of Washington) Report (1998).
[47] S.E. Vigdor, in Future Directions in Particle and Nuclear Physics at Multi-GeV Hadron Beam Facilities, ed. D.F. Geeseman (Brookhaven National Laboratory Report BNL-52389, 1993), p. 171.
[48] M.S. Ball *et al.*, IUCF Internal Report (1994).
[49] COSY Proposal 33, T. Sefzick, spokesperson.
[50] T. Kishimoto, Nucl. Phys. A629, 369c (1998).
[51] J. Haidenbauer *et al.*, Phys. Rev. C52, 3496 (1995).
[52] A. Parreño *et al.*, Phys. Rev. C59, 2122 (1999).

Table I Weak meson-nucleon couplings constants

Coupling	Theoretical							Experimental	
	range (DDH)	'best value' (DDH)	value (DZ)	range (FCDH)	'best value' (FCDH)	value (D)	value (KM)	best fit	range
f_π	0→11.4	4.6	1.1	0→6.5	2.7	2.7	0.19	2.3	0→11
h_ρ^0	-31→11.4	-11.4	-8.4	-31→11	-3.8	-6.1	-1.9	-5.7	-31→11
h_ρ^1	-0.38→0	-0.19	0.38	-1.1→0.4	-0.4	-0.4	-0.02	-0.2	-0.4→0.0
h_ρ^2	-11.0→-7.6	-9.5	-6.8	-9.5→-6.1	-6.8	-6.8	-3.8	-7.6	-11→-7.6
h_ω^0	-10.3→5.7	-1.9	-3.8	-10.6→2.7	-4.9	-6.5	-3.8	-4.9	-10→5.7
h_ω^1	-1.9→-0.8	-1.1	-2.2	-3.8→-1.1	-2.3	-2.3	-1.0	-0.6	-1.9→-0.8

Table II Comparison of calculated and measured sensitivities to systematic errors and the precision required in measuring the various parameters.

Beam Parameter	Sensitivity (calculated)	Sensitivity (measured)	Measure to
$< xP_y >$	$+3 \times 10^{-5}$ mm^{-1}	$+5 \times 10^{-5}$ mm $^{-1}$	12×10^{-5} mm
$< yP_x >$	-3 $\times 10^{-5}$ mm^{-1}	-8 $\times 10^{-5}$ mm^{-1}	8×10^{-5} mm
Position Modulation ($< x > \Delta x$)	3.2 $\times 10^{-5}$ mm^{-2}	1.2 $\times 10^{-4}$ mm^{-2}	5 $\times 10^{-5}$ mm^2
Size modulation	6.5 $\times 10^{-5}$ mm^{-2}	2.9$\times 10^{-4}$ mm^{-2}	3 $\times 10^{-5}$ mm^2
Energy Modulation	1.4 $\times 10^{-8}$/eV	(1.5 $\pm$ 0.2) $\times$ 10 $^{-8}$/eV	0.4 eV
Current Modulation	3 $\times 10^{-9}$ (for $\Delta I/I = 10^{-5}$)	5 $\times 10^{-9}$ (for $\Delta I/I \times 10^{-5}$)	1.0 $\times 10^{-5}$

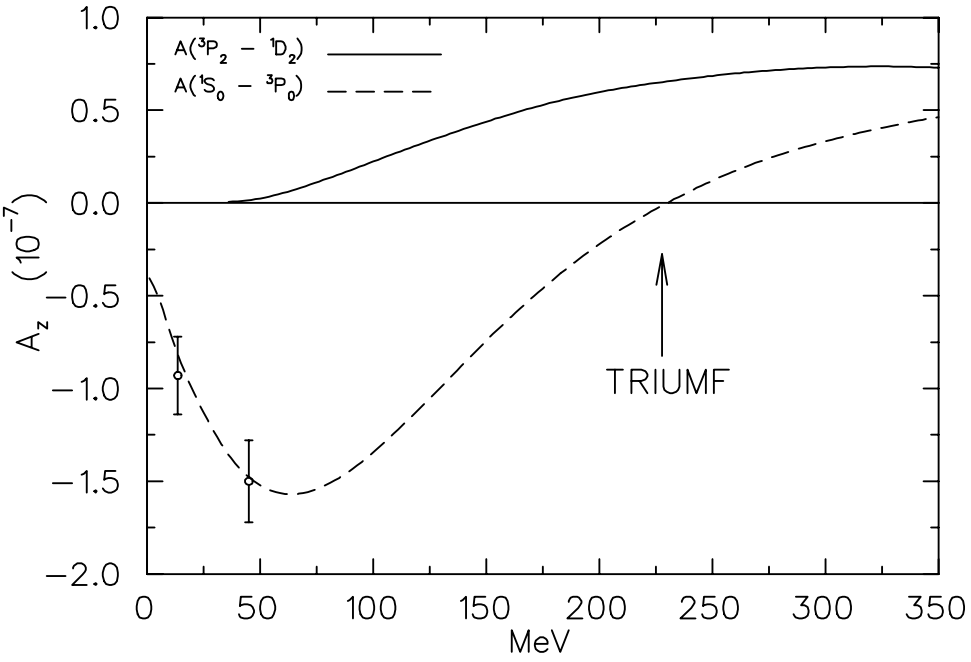

Fig. 1. Contributions to A_z of the first two parity violating transitions in $p-p$ scattering as function of energy.

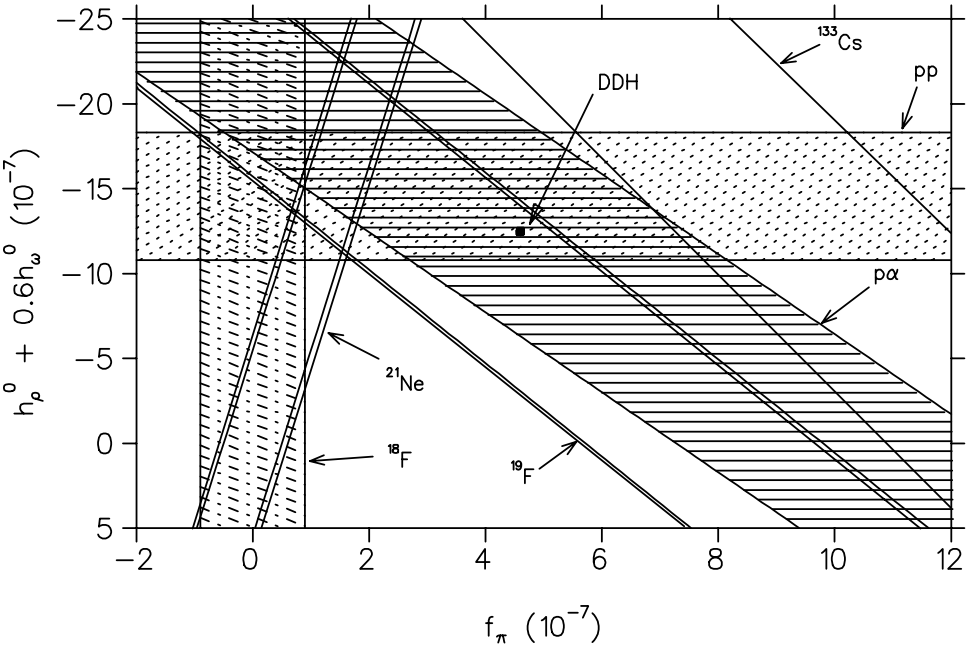

Fig. 2. Plot of the constraints on the isoscalar and isovector weak meson- nucleon coupling constants.

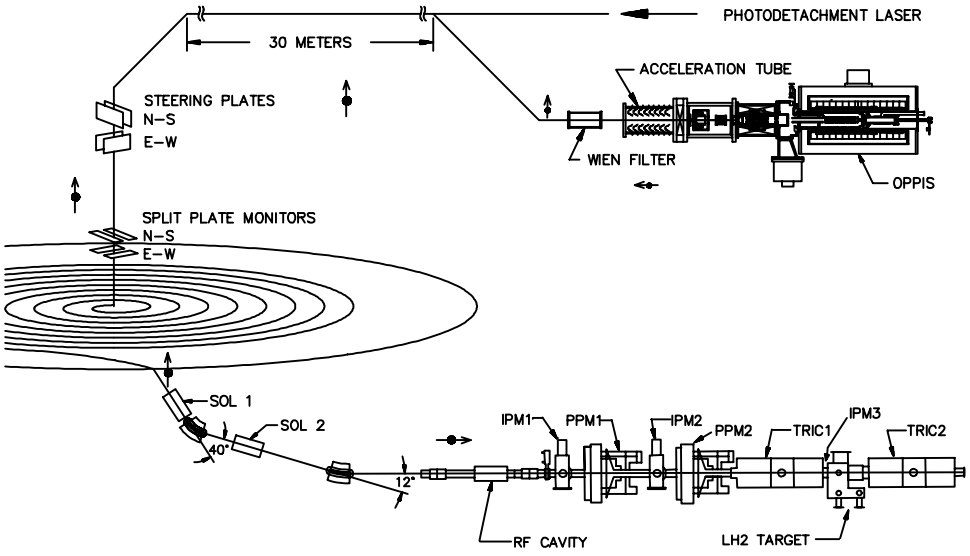

Fig. 3. General layout of the TRIUMF $p-p$ parity violation experiment. (OPPIS: Optically Pumped Polarized Ion Source; SOL: spin precession solenoid magnet; IPM: Intensity Profile Monitor; PPM: Polarization Profile Monitor; TRIC: Transverse Electric field Ionization Chamber). One of eight possible spin directions is indicated.

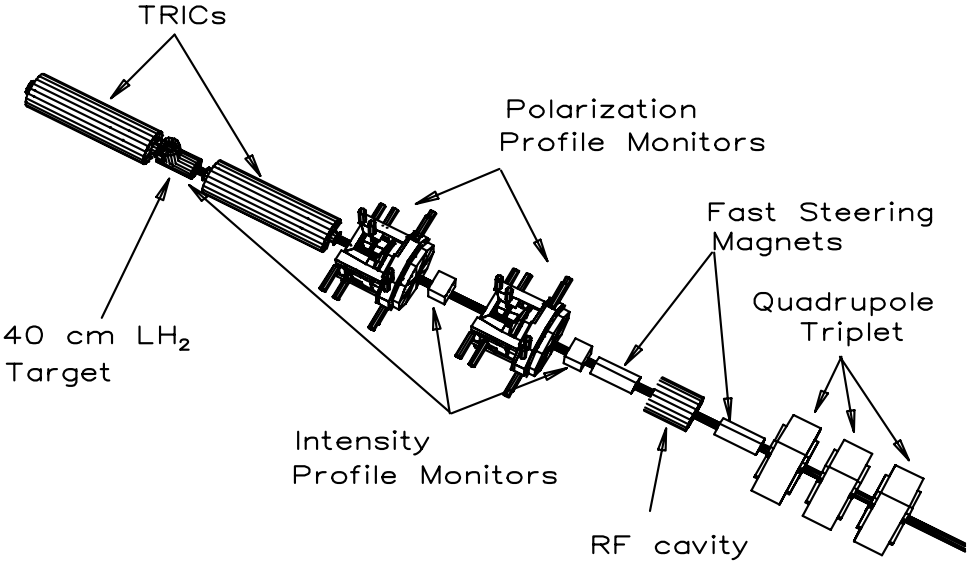

Fig. 4. Three dimensional view of the TRIUMF $p-p$ parity violation detection apparatus. (note the beam entering from the lower right)

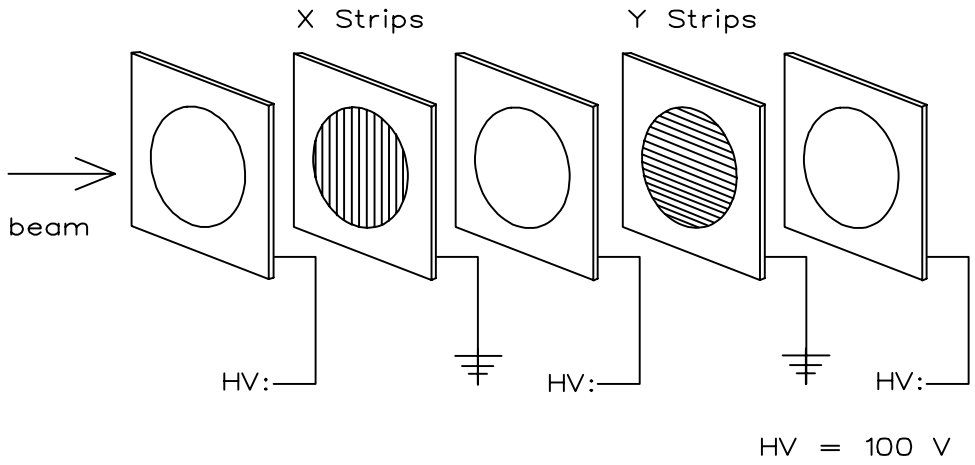

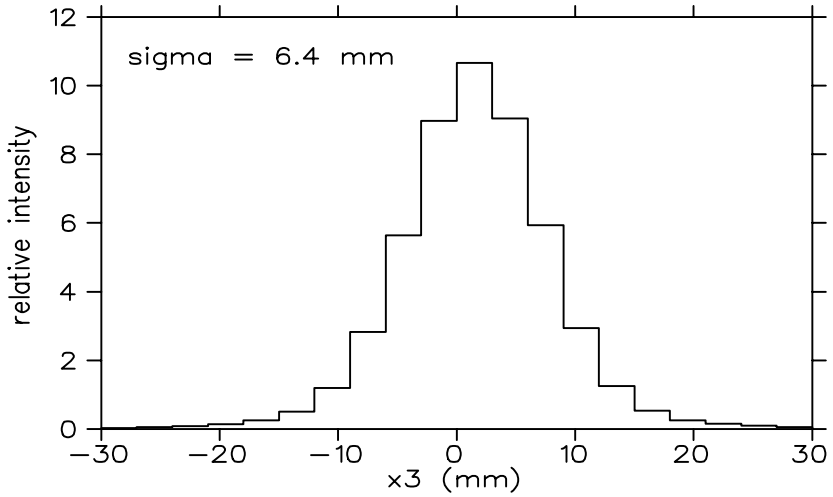

Fig. 5. a) Schematic representation of the assembly of foil harps of each IPM. The foil harps are mounted on G10 frames with apertures of 76 mm (for IPM-3 140 mm). b) Typical horizontal beam intensity profile produced by a harp of 31 aluminium strips (3.00 mm center to center) of IPM-3. The intensity profile has a σ_x of 6.4 mm.

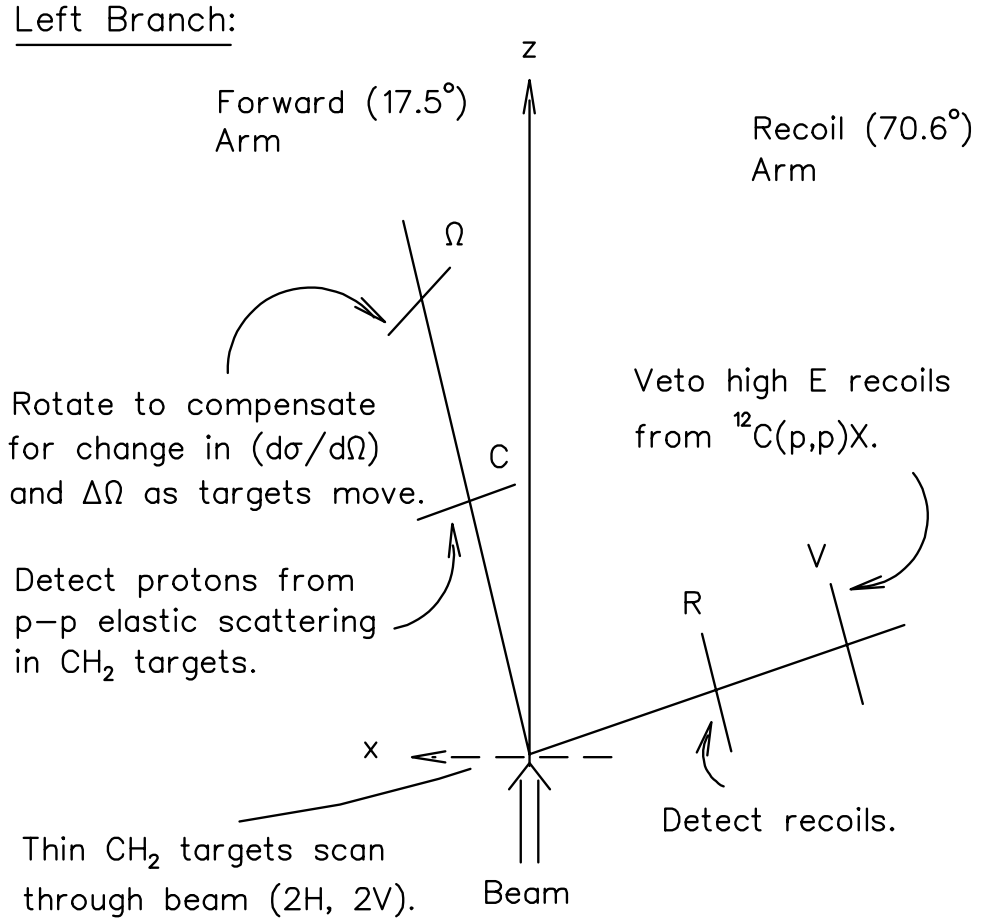

Fig. 6. Schematic representation of one of the four detector assemblies of each PPM.

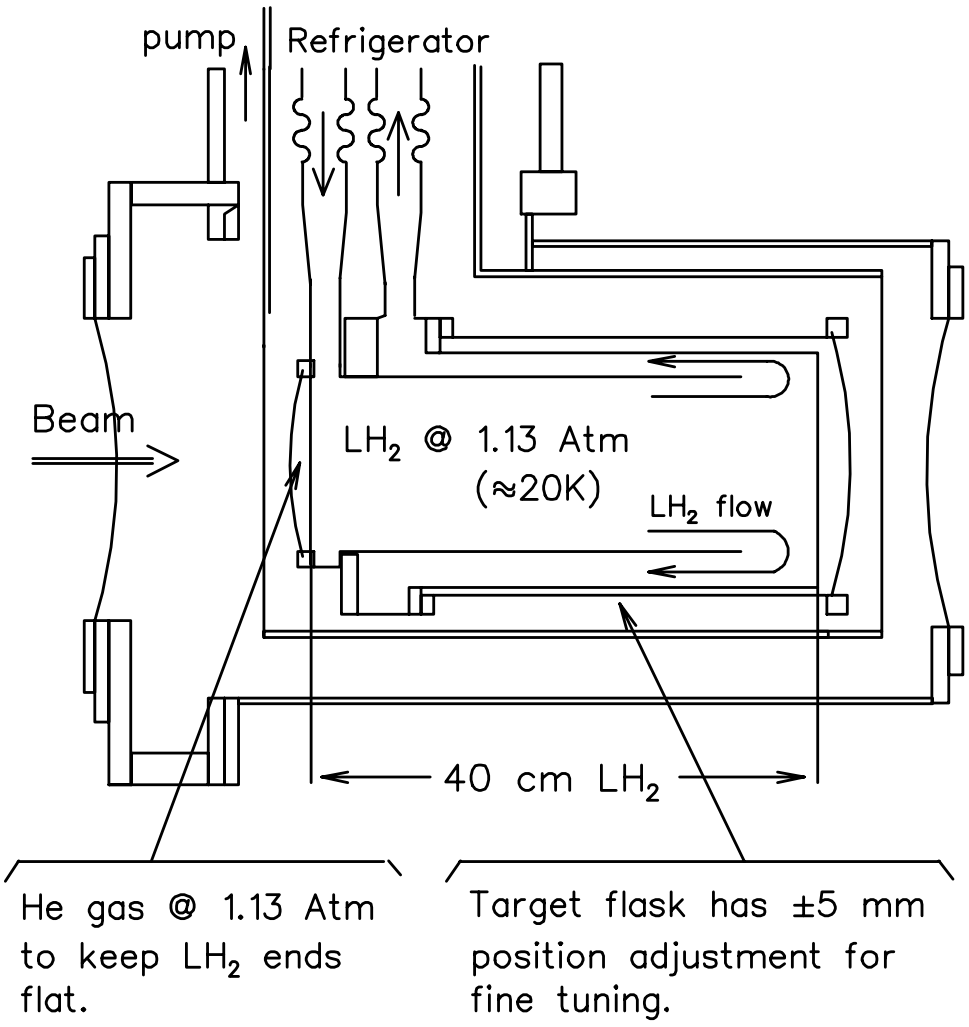

Fig. 7. Engineering drawing of the LH_2 target.

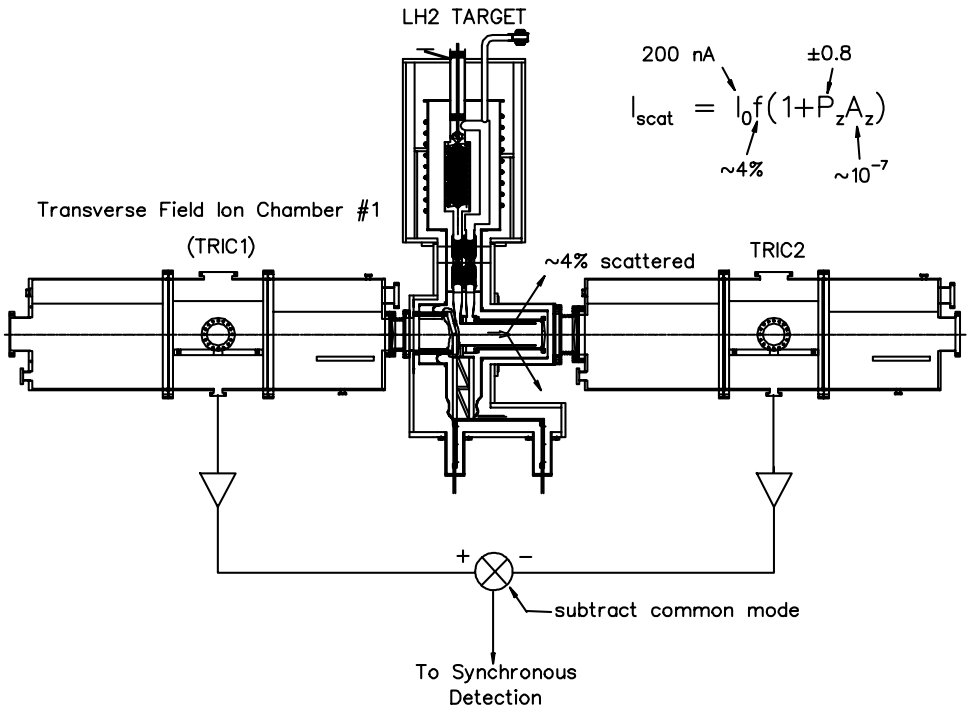

Fig. 8. Parity violation data taking apparatus: TRIC1 and TRIC2 are the transverse electric field ionization chambers with a 0.60 m long by 0.15 m wide by 0.15 m high sense region and contain ultrapure hydrogen gas at approximately 150 torr pressure; the LH_2 target is 0.40 m long.

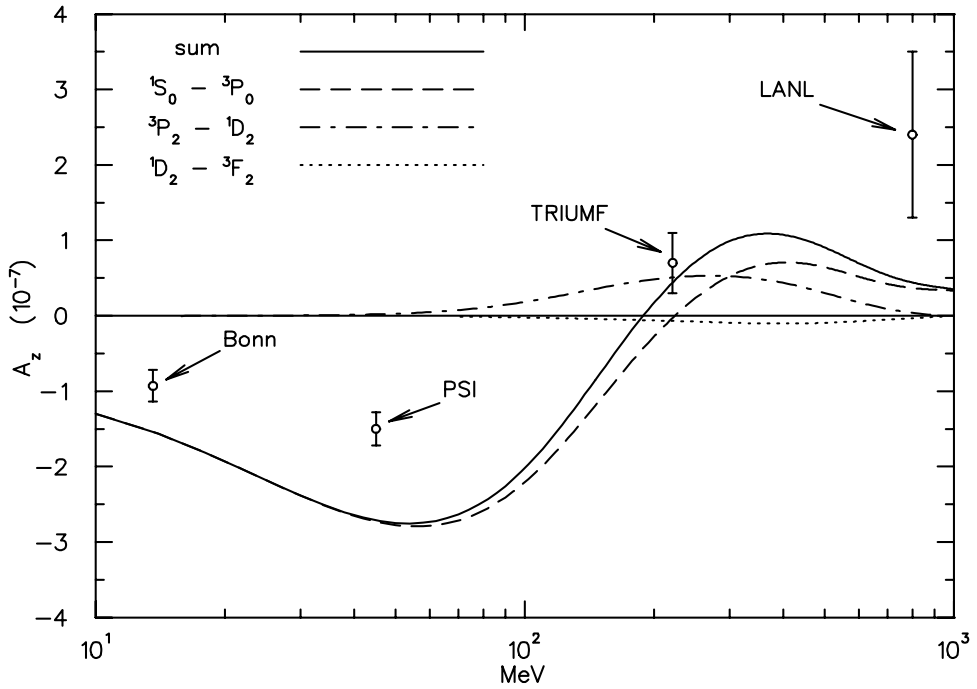

Fig. 9. Energy dependence of the $p - p$ parity violating longitudinal analyzing power A_z. The curves give the total and the individual contributions of the first three parity violating transition amplitudes as calculated by Driscoll and Miller [Ref.33] in a weak meson exchange model. Note the logarithmic energy dependence of the abscissa. The 221 MeV datum is a partial result of the TRIUMF experiment.

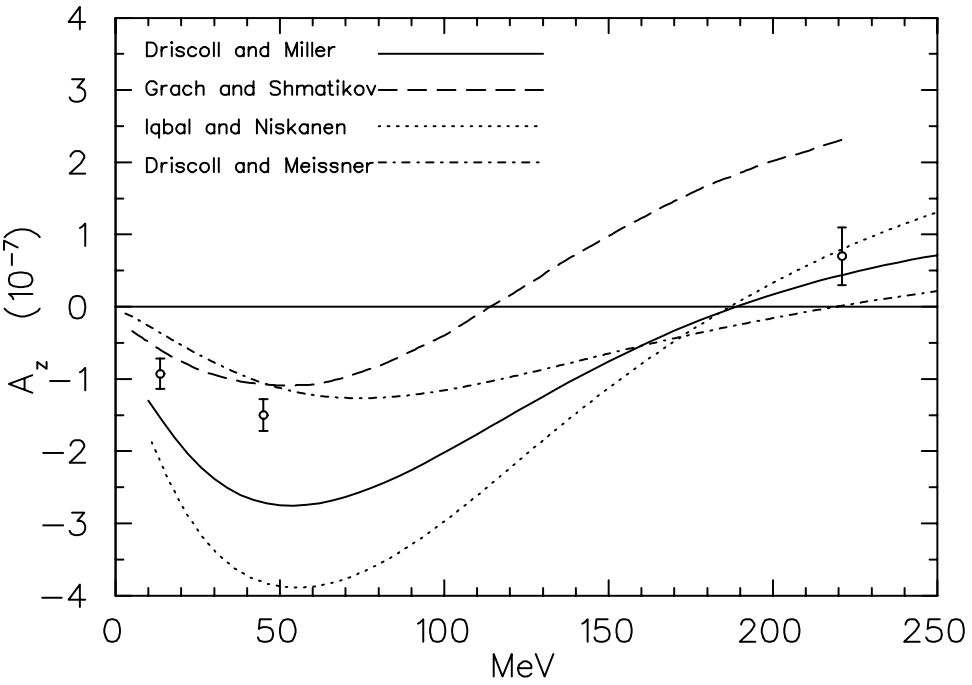

Fig. 10. Theoretical predictions by Driscoll and Miller [Ref. 33], Grach and Shmatikov [Ref. 37], Iqbal and Niskanen [Rev. 32], and Driscoll and Meissner [Ref. 34] and the low energy $p-p$ parity violating longitudinal analyzing power (A_z) data.

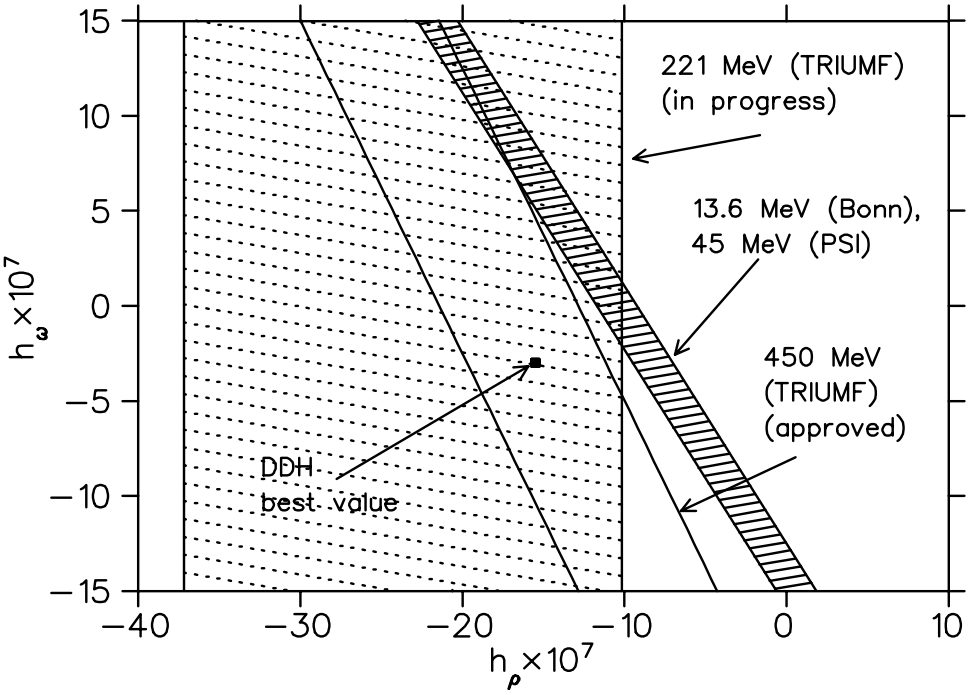

Fig. 11. Plot of the constraints placed on the weak meson-nucleon coupling constants by the $p-p$ parity violation experiments. The limit placed by the low-energy measurements is shaded; the DDH "best value" is indicated. The error of a 450 MeV measurement is assumed to be $\pm 2 \times 10^{-8}$.

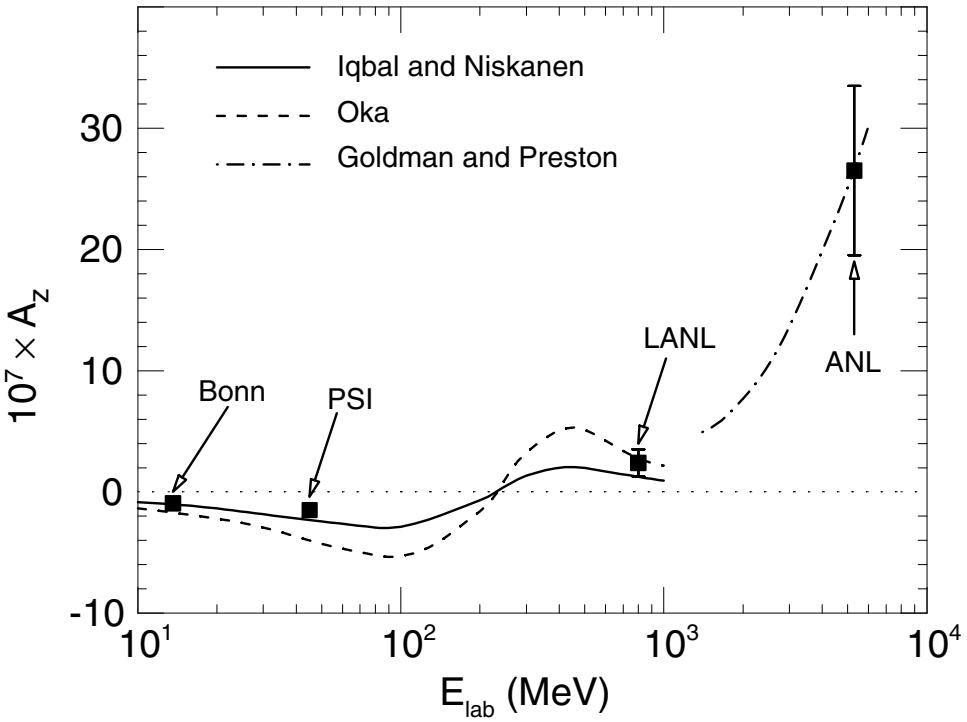

Fig. 12. Energy dependence of the $p - p$ parity violating longitudinal analyzing power in the energy range 10 MeV to 10 GeV. The solid and dashed curves are from Iqbal and Niskanen [Ref. 32] and Oka [Ref. 45], respectively, based on weak meson exchange models; the dot-dashed curve is from Goldman and Preston [Ref. 42] and is described in the text.

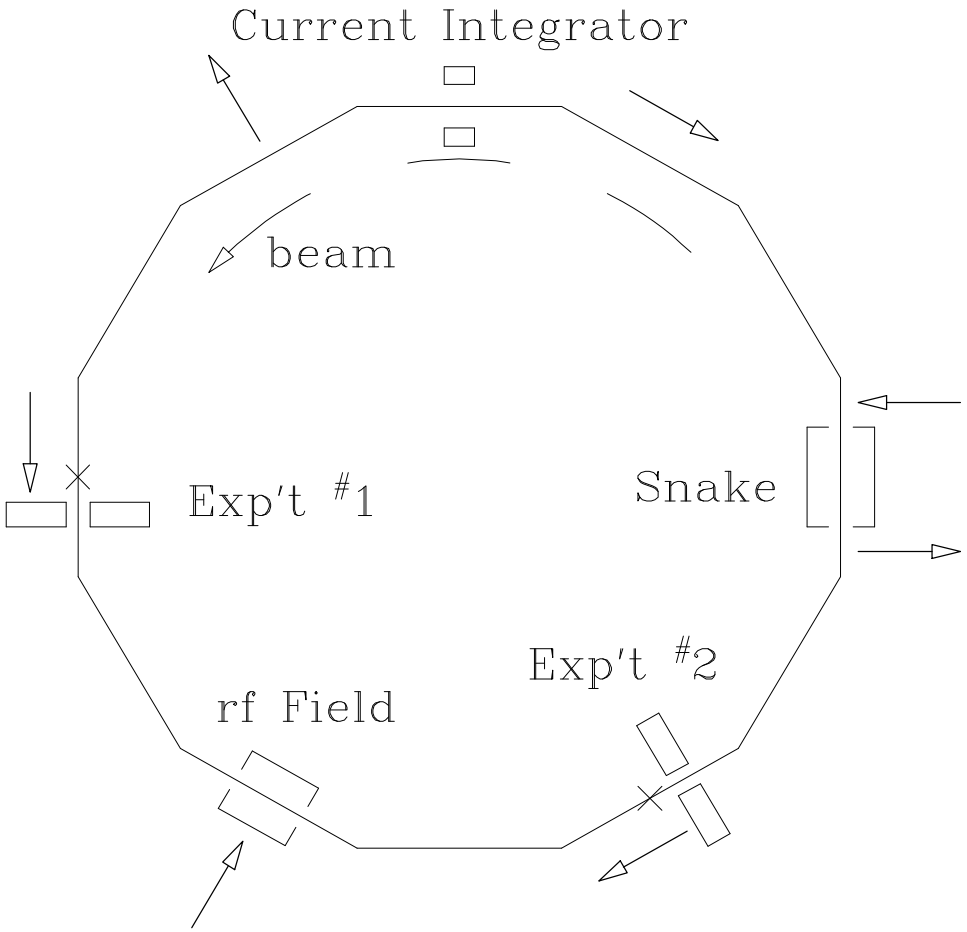

Fig. 13. Schematic layout of a possible $p-p$ parity violation experiment in a storage ring with internal targets. The target for a transmission (attenuation) experiment would be mounted at the location labeled 'Exp't #1'. Note the location of the Siberian snake of the first kind (figure is from reference 47).